

# Residue Theorem Based Sensorless Maximum Power Point Tracking Tip Speed Ratio Control for Wind Generation System

Mohammed Alsumiri, Lin Jiang, and Sami Alalwani

**Abstract**—This research proposes a direct sensorless Maximum Power Point Tracking (MPPT) Tip Speed Ratio (TSR) control based on wind speed and rotor speed estimation for Wind Generation System (WGS) with direct driven Permanent Magnetic Synchronous Generators (PMSG). Also in this paper, a new improved technique to estimate the rotor speed using back-EMF is introduced. The new technique is designed based on the mathematical residual theorem. The controller uses an estimated wind speed data derived from electrical measurements of voltage and current along with the previously estimated PMSG rotational speed. Using rotational and wind speeds estimated data, the TSR is obtained using calculation method and set side to side to its optimal value. The proposed controller uses only the stator currents and voltages measurements to control the WGS. The validation of the proposed controller is shown by MATLAB/SIMULINK simulation.

**Index Terms**—Back-EMF observer, Maximum power point tracking, PMSG control, Residue, Wind generation system, Wind speed estimation algorithm.

## I. INTRODUCTION

THE generated electrical energy which is extracted from wind power depends on the amount of available power in the wind and the control strategy of WGS. For small-scale low-cost applications it is recommended to use PMSG with variable speed operation [1]. One advantage of the variable speed operation is the ability to keep a maximum conversion of power exists under different wind speeds. The MPPT algorithm objective is to obtain TSR at its optimum value, which insures the maximum capture of power under different conditions.

A nonlinear control theory improves the performance and the speed achievement to the tracked maximum power point speed [2]. In order to achieve a high performance controller mechanical speed sensors are required. Most sensorless controller techniques are unstable at low speed since the estimation techniques are parameter dependent. Several methods have been reported using high frequency signal injection neglecting the back-EMF and the stator resistance where the speed and position is estimated using the variations of the machine inductance [3], [4], [5]. A sensorless rotor position and wind speed control for PMSG based WGS was developed in [6]. The rotor position was estimated using a sliding-mode observer, which uses the stator currents measurements and the voltages were obtained from the machine-

side converter controller. [7] provided a solution to deal with the unknown wind speeds. The wind speed is estimated using the efficiency curve of the blade.

A soft sliding mode control based on residue theorem has been proposed in [8]. The new control strategy redefines the error as the residual value between the controlled variable and the set point. The successful achievement of improving the system dynamics and efficiency came from the idea of creating a dynamic boundary for the error.

The rotor speed is estimated in this research using improved back-EMF observer. The improved back-EMF observer uses the residual value of the back-EMF rather than the calculated value. The idea is to create a boundary around the exact calculated value and the residual value lies under this boundary. The calculated value is then compared with previous residual value. In addition, the wind speed is estimated using the wind power model and the calculated AC power. The MPPT controller generates a reference speed corresponds to an optimal TSR which insures the maximum power conversion. The residual value of the TSR is compared to the optimal value of TSR and the error is used to generate a PWM signal to control the switching of the DC-DC boost converter. This paper is organized as follows. In section II an introduction of the mathematical residue theorem and the forward Euler method are presented. Also, this section includes the wind turbine model. In section III the improved back-EMF observer is designed. The design of the wind speed estimator is shown in section IV. In section V, the MPPT algorithm is explained and implemented to the WGS. Section VI presents the simulation results and analysis where section VII is the conclusion.

## II. MATHEMATICS AND SYSTEM OVERVIEW

### A. Residue Theorem

Residue theorem is nominated to be a powerful tool in prediction of the area under a curve. It has been declared by The Cauchy Theorem that whenever a function is analytic on and in a closed contour  $C$ , then the integral over the closed contour is zero [9], [10].

*Cauchy's Residue Theorem 1:* Let  $D$  be a simply connected domain, and let  $C$  be a simple closed positively oriented contour that lies in  $D$ . If  $f(z)$  is analytic inside and on  $C$ , except at the points  $z_1, z_2, \dots, z_n$  that lie inside  $C$  [11]-[12], then

$$\oint_C f(z) dz = 2\pi i \sum_{k=1}^n \text{RES}[f, z_k]. \quad (1)$$

Manuscript received July 15, 2019; revised August 04, 2019.

Mohammed Alsumiri and Sami Alalwani are with the Department of Electrical and Electronics Engineering, Yanbu Industrial College, Yanbu, Saudi Arabia e-mail: (alsumiri@rcyci.edu.sa).

Lin Jiang is with the Department of Electrical Engineering and Electronics, University of Liverpool, Liverpool, UK.

The above situation can be illustrated graphically as in Fig. 1 [11]. The generalized expression for the residue theorem could be written as in the below equation (2).

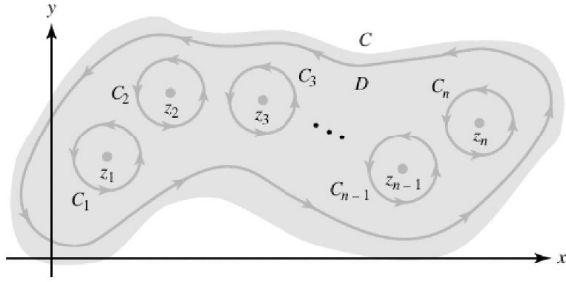


Fig. 1: Representation of Cauchy's Residue Theorem

$$RES f(x) = \frac{1}{2\pi i} \int_{-\infty}^{+\infty} f(x) dx. \quad (2)$$

For operating point convergence assurance to the desired point, the forward Euler method is fulfilled. Therefore the stability of the operating point is sustained By assuring the convergence of the operating point. Considering a controlled variable  $y$  and a step size of  $h$ , the forward Euler method can be expressed as below,

$$\dot{y} \approx \frac{y(t+h) - y(t)}{h}. \quad (3)$$

### B. System Description

The configurations of the investigated WGS is demonstrated in Fig. 2. The WGS has a PMSG which is directly driven by a vertical axial wind turbine (VAWT). The generated AC voltage is rectified using a three phase uncontrolled diode rectifier circuit. The DC voltage level is then boosted and controlled through a continuous mode operated DC/DC boost converter.

### C. Wind Turbine Model

It is well known that wind turbines extract the stored kinetic energy from the wind and convert it to rotational energy in order to drive the alternator. However, the amount of available power in the wind is a function of the cube of wind speed [13].

$$P_w = \frac{1}{2} \rho A V_w^3, \quad (4)$$

where  $\rho$  demonstrates the density of air,  $V_w$  represents meter per second speed of the wind and  $A$  is the wind turbine swept area. The possible rotational power which is extracted from the wind power is governed by a power coefficient  $C_p$  as below:

$$P_m = \frac{1}{2} \rho C_p A V_w^3. \quad (5)$$

The exact approximation of a power coefficient is built upon wind turbine, i.e. horizontal or vertical axial type. The blade's pitch angle as well as the tip speed ratio ( $\lambda$ ) are used to obtain the approximated value of  $C_p$ . In most cases this value is already obtained and provided by wind turbine

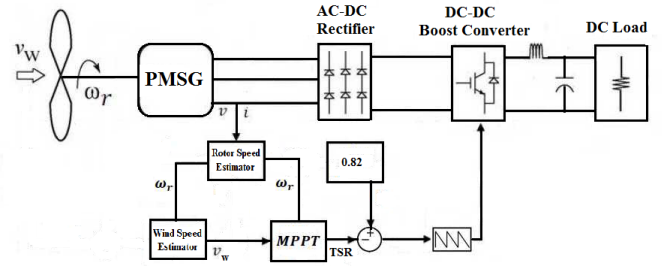


Fig. 2: Wind generator system description and control

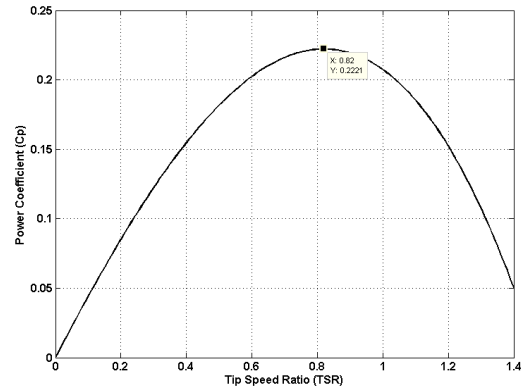


Fig. 3: Power coefficient versus TSR

manufacturer. However for further investigation and accuracy several polynomials were found out taking into account the pitch angle [14]. It has been reported that for small-scale low-cost applications, it is preferred to avoid pitch angle control and use a fix pitch angle. Succseded in doing so reducing the extra cost caused by controlling the pitch angle. The relationship between  $C_p$  and  $\lambda$  can be shown as follows [13]:

$$C_p = -0.13\lambda^3 - 0.12\lambda^2 + 0.45\lambda, \quad \lambda = \frac{\omega_r R}{V_w}, \quad (6)$$

where  $R$  represent the wind turbine rotor radius,  $\omega_r$  demonstrate the mechanical speed. By solving equation 6 for a TSR from 0 to 2, the  $C_p$  versus TSR curve can be shown in Fig 3. It is noticeable that the WGS can maintain maximum extraction from the available power in the wind at 0.82 TSR.

### III. IMPROVED BACK-EMF OBSERVER USING RESIDUE THEOREM

Several techniques in observing the back-EMF for rotational speed estimation have been reviewed in [15]. The developed observer in this research is an improved back-EMF observer based on mathematical residue theorem. The approach is to use the residual value of the back-EMF rather than using the back-EMF value to estimate rotor speed. The demonstrations of the sinusoidal back-EMF equations in the  $\alpha - \beta$  co-ordinate are as the followings [8]:

$$\begin{aligned} e_\alpha &= L \frac{d}{dt} i_\alpha + R_a i_\alpha + V_\alpha, \\ e_\beta &= L \frac{d}{dt} i_\beta + R_a i_\beta + V_\beta, \end{aligned} \quad (7)$$

where  $e_{\alpha\beta}$  represents the coordinates back-EMF,  $V_{\alpha\beta}$  are the coordinates terminal voltages and  $i_{\alpha\beta}$  represents the

coordinates currents.  $L$  represents the inductance of the PMSG. In classical back-EMF observer, an estimation of  $\theta$  which is the rotor position could be obtained from (7) as,  $\hat{\theta} = \tan^{-1} \left( \frac{e_\alpha}{e_\beta} \right)$  [16]. The implementation of the residue theorem in the back-EMF observer can be done following two stages. The first stage is to define the error according the forward Euler equation 3. The error  $e$  is the deference between the actual back-EMF minus the previous value of the back-EMF. The new error  $e_e$  equation can be defined as follows, where  $c$  is a constant:

$$\begin{aligned} \dot{e}_e &= e + c, \\ e_e &= \int e + c, \\ e_e &= \frac{e^2}{2} + ce. \end{aligned} \quad (8)$$

The second stage is to define the boundary in which the back-EMF lies on. In this paper the back-EMF value is bounded by its value plus and minus the error. The proposed improved back-EMF observer can be shown as the following:

$$\begin{aligned} \hat{e}_{\alpha\beta} &= RES(e_{\alpha\beta}), \\ \hat{e}_{\alpha\beta} &= \frac{1}{2\pi} \int_{e_{\alpha\beta}-e_e}^{e_{\alpha\beta}+e_e} e_{\alpha\beta}, \\ \hat{e}_{\alpha\beta} &= \frac{e_{\alpha\beta}e_e}{\pi}, \end{aligned} \quad (9)$$

where  $\hat{e}_{\alpha\beta}$  is the residual value of the back-EMF. In order to achieve a better performance, a low pass filter is introduced in the back-EMF observer with  $200\mu s$ .

#### IV. WIND SPEED ESTIMATION

A famous argument in controlling WGS is the data of the wind speed. It can be very costly and little accurate when using wind speed measurement systems. It has been reported that to improve the accuracy of wind speed data, several anemometer have to be employed [17]. It is well known that the wind speed data obtained from SCADA recording system have obvious deviations. Such mismatch of the wind speed data create diveation in conversion efficiency [18]. The wind speed data obtained in this research are estimated. The developed WGS model that is demonstrated in equations 5 and 6 are solved for as function of wind speed then  $P_m$  is considered as the generated AC power. The estimation equation for wind speed is as below:

$$V_w = \frac{-D_{21}\omega_r^2 \pm \sqrt{D_{21}^2\omega_r^4 - 4D_{11}\omega_r(D_{31}\omega_r^3 - VI)}}{2D_{11}\omega_r}. \quad (10)$$

where  $D_{11} = 0.0960$ ,  $D_{21} = -0.0098$  and  $D_{31} = -0.0040$ .

#### V. MAXIMUM POWER POINT TRACKING USING RESIDUE THEOREM

The MPPT can be achieved by controlling the TSR to its optimum value  $\lambda_{opt}$  which is 0.82. The estimated values of the rotor speed and wind speed are used to calculate TSR. The TSR is then compared with the optimum value and the error is defined using residue theorem. The MPPT algorithm using residue theorem can be express as below:

TABLE I: WGS Name Plate Parameters

Parameters	Value
VAWT	
Type	VAWT Savonius
Output Power	165 W
$C_p$	0.22
Optimum Tip Speed Ratio	0.82
Permanent Magnet Synchronous Generator	
Type	GL-PMG500A
output Power	500 W
internal Resistance	0.35 $\Omega$
Moment of Inertia	0.066Kg.m <sup>2</sup>

$$\begin{aligned} \lambda &= \frac{\omega_r R}{V_w}, & \lambda_{opt} &= 0.82, \\ e_\lambda &= \lambda_{opt} - \lambda, & \dot{e}_k &= e_\lambda + k, \\ \hat{\lambda} &= \frac{1}{2\pi} \int_{\lambda_{opt}-e_k}^{\lambda_{opt}+e_k} \lambda, \\ \hat{\lambda} &= \frac{\lambda_{opt}e_k}{\pi}, \end{aligned} \quad (11)$$

where  $e_\lambda$  and  $e_k$  are the TSR error and the new TSR which is defined by the forward Euler method respectively.  $k$  is a constant.

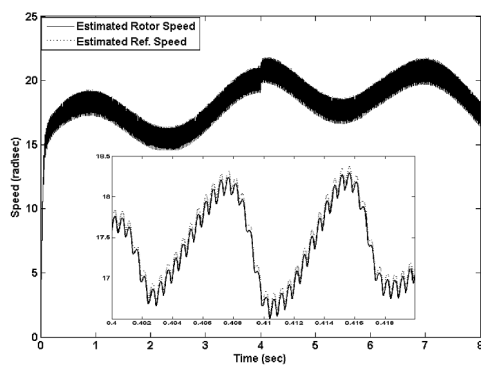
#### VI. SIMULATION ANALYSIS AND RESULTS

The control diagrams of the proposed MPPT controller is illustrated in Fig. 2. For the proposed MPPT controller the stator voltages and currents are measured then the power is calculated. The measured data is used to estimate the rotation speed using an improved back-EMF observer by implementing the residue theorem. The estimated rotating speed as well as the calculated power is used to estimate the wind speeds. Both the estimated speeds are used to obtain a MPPT operation by calculating the TSR and compare the results to the optimum TSR and the error signal is used for controlling the PWM boost DC-DC converter operation.

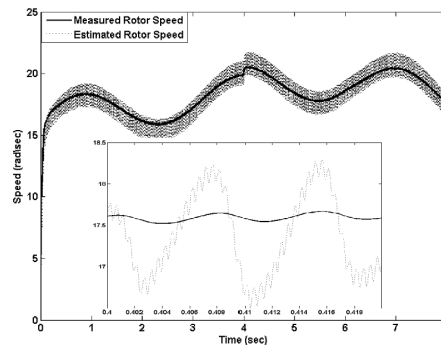
The developed model of the investigated wind turbine is based on a VAWT type coupled directly to a PMSG. The simulations of WGS model were carried out based on fluctuated wind speeds. The wind function fluctuates between 8 – 10 m/s that emulates real wind speed profile. Table I shows the employed wind turbine and generator parameters.

The MPPT controller has been modelled and tested via MATLAB/SIMULINK simulation enviroment. The integration effect, which appears in the residue equation, makes the boundary limits changing in a soft manner. Figures 4a shows the rotational speed following its reference obtained using estimations. It is determined that the estimated speed follows its reference value from MPPT perfectly with smooth dynamics that are free from overshoots. In addition, the accuracy in achieving the desired value eliminates steady-states error. In further investigations the dynamics shows fast response and satisfactory settling time.

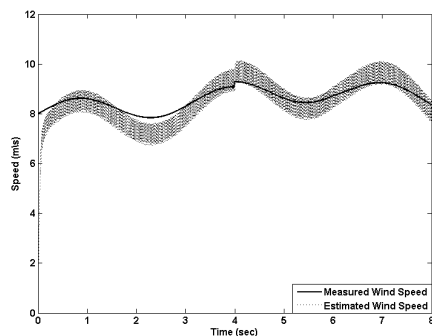
Figure 4b illustrates the real measured rotor speed following the speed obtained by the estimator. It is clearly shown that the estimated rotor speed is very close to the measured rotor speed. According to the fact that the back-EMF observer has a poor performance at low speeds, the results shows an acceptable performance for the improved



(a) Estimated speed tracking the Estimated reference speed.



(b) Comparison between speeds obtained from measurement and estimated.



(c) Comparison between Measured and estimated wind speeds.

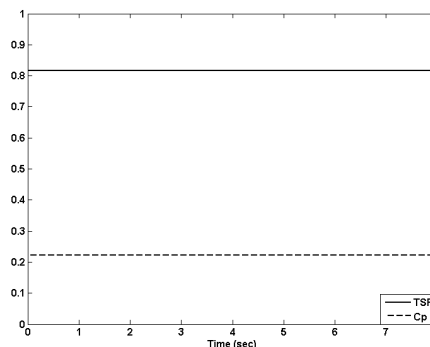

 (d) TSR and  $C_p$ .

Fig. 4: Simulation result for the proposed MPPT controller

back-EMF observer at low speed. Moreover it can be noted that the estimated speed varies quickly and smoothly when the wind speed is changing.

Figure 4c shows a comparison between the measured wind speed and estimated wind speed. It is clear from the figure that the estimated wind speed accurately matches the measured wind speed. Furthermore, the dynamic speed is quite fast as well as settling time to the desired value. The TSR and  $C_p$  shown in Fig.4d indicate their optimal values at 0.82 and 0.221 respectively.

## VII. CONCLUSION

Summarizing this research, a residue theorem based novel sensorless MPPT controller has been proposed. The idea is to observe the residual value of the back-EMF rather than the classical back-EMF. The rotational speed is estimated based on the residual back-EMF observations. In fact, this technique improves the speed estimation for low speed operations. Moreover, the wind data has been obtained using an estimation to improve the wind data accuracy and reduces the cost for low cost applications. The strong point is that the uncertainty of the data is handled by the controller perfectly. The stability has been assured by employing the forward Euler method which assures that the point is converted to its desired value. The proposed controller has been tested and investigated via simulations. The results show strongly accepted responses. The dynamics are free of overshoot at fast speed. It can be concluded that using the residual value of the back-EMF gives a better observer performance especially at low speed operations. Moreover, it can be highlighted that a sensorless TSR control improves the WGS dynamics.

## REFERENCES

- [1] C. Xia, Q. Geng, X. Gu, T. Shi, and Z. Song, "Input-output feedback linearization and speed control of a surface permanent-magnet synchronous wind generator with the boost-chopper converter," *IEEE Transactions on Industrial Electronics*, vol. 59, no. 9, pp. 3489–3500, 2012.
- [2] K. Khadija, M. Benyounes, B. I. Khalil, and B. M. Rachid, "A simple and robust speed tracking control of pmsm," *Przeglad Elektrotechniczny*, vol. 87, no. 7, pp. 202–207, 2011.
- [3] G. M. El-Murr, D. Giaouris, and J. W. Finch, "Sensorless speed estimation of pmsm near zero speed using online short time fourier transform ridges," in *World Congress on Engineering*, 2007, pp. 481–485.
- [4] J.-H. Jang, S.-K. Sul, J.-I. Ha, K. Ide, and M. Sawamura, "Sensorless drive of surface-mounted permanent-magnet motor by high-frequency signal injection based on magnetic saliency," *Industry Applications, IEEE Transactions on*, vol. 39, no. 4, pp. 1031–1039, 2003.
- [5] Y.-s. Jeong, R. D. Lorenz, T. M. Jahns, and S.-K. Sul, "Initial rotor position estimation of an interior permanent-magnet synchronous machine using carrier-frequency injection methods," *Industry Applications, IEEE Transactions on*, vol. 41, no. 1, pp. 38–45, 2005.
- [6] W. Qiao, X. Yang, and X. Gong, "Wind speed and rotor position sensorless control for direct-drive pmg wind turbines," *Industry Applications, IEEE Transactions on*, vol. 48, no. 1, pp. 3–11, 2012.
- [7] H.-S. Shin, C. Xu, J.-M. Lee, J.-D. La, and Y.-S. Kim, "Mpppt control technique for a pmsg wind generation system by the estimation of the wind speed," in *Electrical Machines and Systems (ICEMS), 2012 15th International Conference on*. IEEE, 2012, pp. 1–6.
- [8] M. Alsumiri, L. Li, L. Jiang, and W. Tang, "Residue theorem based soft sliding mode control for wind power generation systems," *Protection and Control of Modern Power Systems*, vol. 3, no. 1, p. 24, 2018.
- [9] J. Bak and D. J. Newman, *Complex analysis*. Springer, 2010.
- [10] E. Cattani and A. Dickenstein, "Introduction to residues and resultants," in *Solving polynomial equations*. Springer, 2005, pp. 1–61.
- [11] R. H. Nevanlinna and V. Paatero, *Introduction to complex analysis*. American Mathematical Soc., 1969, vol. 310.
- [12] I. N. Bronshtein, K. A. Semendiaev, and K. A. Hirsch, *Handbook of mathematics*. Van Nostrand Reinhold New York, 1985.
- [13] T. Burton, N. Jenkins, D. Sharpe, and E. Bossanyi, *Wind energy handbook*. Wiley, 2011.

- [14] S. Morimoto, T. Nakamura, and Y. Takeda, "Power maximization control of variable speed wind generation system using permanent magnet synchronous generator," *IEEE Transactions on Power and Energy*, vol. 123, pp. 1573–1579, 2003.
- [15] Y. Zhao, C. Wei, Z. Zhang, and W. Qiao, "A review on position/speed sensorless control for permanent-magnet synchronous machine-based wind energy conversion systems," *IEEE Journal of Emerging and Selected Topics in Power Electronics*, vol. 1, no. 4, pp. 203–216, 2013.
- [16] Y. Zhao, W. Qiao, and L. Wu, "Position extraction from a discrete sliding-mode observer for sensorless control of ipmsms," in *Industrial Electronics (ISIE), 2012 IEEE International Symposium on*. IEEE, 2012, pp. 725–730.
- [17] S. El Aïmani, "Modeling and control structures for variable speed wind turbine," in *Multimedia Computing and Systems (ICMCS), 2011 International Conference on*. IEEE, 2011, pp. 1–5.
- [18] Y. Wang, D. G. Infield, B. Stephen, and S. J. Galloway, "Copula-based model for wind turbine power curve outlier rejection," *Wind Energy*, 2013.